Supplementary Information

Synthesis and Self-assembly of Diblock Glycopolypeptide Analogues PMAgala-*b*-PBLG as Multifunctional Biomaterials for Protein Recognition, Drug Delivery and Hepatoma Cell Targeting

Zhao Wang[1], Ruilong Sheng[1,2]*, Ting Luo[1], Jingjing Sun[1], Amin Cao[1]*

1.CAS Key Laboratory of Synthetic and Self-assembly Chemistry for Organic Functional Molecules, Shanghai Institute of Organic Chemistry, Chinese Academy of Sciences, 345 Lingling Road, Shanghai 200032, China

2. Department of Chemistry, Université de Montréal, Succursale Centre-ville, Montreal, Quebec, H3C3J7, Canada.

Fig. S6 TEM images for the self-assembled micelles prepared by PMAgala$_{27}$-*SS*-PBLG$_{27}$ (A), PMAgala$_{27}$-*SS*-PBLG$_{40}$ (B), PMAgala$_{27}$-*SS*-PBLG$_{50}$ (C) and PMAgala$_{27}$-*CC*-PBLG$_{30}$ (D).

Fig. S7 CD spectra for the PMAgala-*b*-PBLG micelles in deionized water (A) and featured FTIR spectra (B) for the freeze-dried powders from the PMAgala$_{27}$-*SS*-PBLG$_{30}$ micelles solution (blue curve) and solids (red curve).

Fig. S8 Stability assay for the PMAgala$_{27}$-*SS*-PBLG$_{30}$ micelles by DLS in the presence of FBS, BSA, SDS or NaCl. (A) Time dependence of relative light scattered intensity. (B) Particle size change after 24 h incubation.

Fig. S9 Incubation time dependence of relative light scattered intensity and average particle size for the PMAgala$_{27}$-*CC*-PBLG$_{30}$ micelles in the presence of 10 mM GSH at 37℃.

Table S1 Characteristics of the DOX-loaded PMAgala-*b*-PBLG micelles.

S1. Synthesis of azido-functionalized RAFT chain transfer agent CDP-SS-N_3 and CDP-CC-N_3

CDP-SS-N_3 was synthesized in three steps as shown in Scheme S1. Firstly, bromoacetic acid (0.42 g, 3 mmol) dissolved in 50 mL of tetrahydrofuran was added dropwise into a 150 mL flask with 2-hydroxyethyl disulfide (1.39 g, 9 mmol), DCC (1.85 g, 9 mmol) and DMAP (0.11 g, 0.9 mmol) dissolved in 20 mL of tetrahydrofuran. The mixture was kept stirring for 24 h at room temperature, and then filtered and continuously purified by flash column chromatography (eluent: EtOAC/hexane = 1/3, *v/v*) to get 2-((2-hydroxyethyl)disulfanyl) ethyl-2-bromoacetate as white viscous liquid (0.55 g, 67% yield). Secondly, 2-((2-hydroxyethyl)disulfanyl)ethyl-2-bromoacetate (0.55 g, 2 mmol) and sodium azide (0.26 g，4 mmol) were reacted in DMF (10 mL) at 40°C for 30 h. The reaction mixture was cooled to room temperature, poured into ethyl ether (50 mL), and extracted with saturated aqueous NaCl solution (3×50 mL). The organic layer was separated, dried over anhydrous Na_2SO_4, filtered and purified by flash column chromatography (eluent: EtOAC/ hexane = 1/3, v/v) to

get 2-((2-hydroxyethyl)disulfanyl)ethyl-2-azidoacetate as white viscous liquid (0.39 g, 83% yield). Thirdly, 2-((2-hydroxyethyl)disulfanyl)ethyl-2-azidoacetateas (0.39 g, 1.66 mmol), DCC (0.68 g, 3.32 mmol), DMAP (0.61 g, 0.50 mmol) and RAFT chain transfer agent of 4-cyano-4-(dodecylsulfanyl thiocarbonyl) sulfany pentanoic acid (CDP) were dissolved in 30 mL of dichloromethane and reacted at room temperature for 24 h. The reaction mixture was continuously filtered, washed with saturated aqueous NaCl solution (3×30 mL), dried over anhydrous Na_2SO_4, filtered and purified by flash column chromatography (eluent: EtOAC/hexane = 1/5, *v/v*) to finally get azido-functionalized RAFT chain transfer agent CDP-SS-N_3 as yellow viscous liquid (0.63 g, 76% yield).

^{1}H NMR ($CDCl_3$, δ in ppm): 4.47 (t, 2H, COO*CH*$_2$), 4.37 (t, 2H, COO*CH*$_2$), 3.93 (s, 2H, C*H*$_2$N$_3$), 3.33 (t, 2H, C*H*$_2$S), 3.00-2.90 (m, 4H, C*H*$_2$SS), 2.75-2.30 (m, 4H, C*H*$_2$C*H*$_2$C(CN)(CH$_3$)R), 1.89 (s, 3H, C(CN)C*H*$_3$), 1.80-1.50 (m, 4H), 1.28 (br, 18H), 0.89 (t, 3H, C*H*$_3$)

^{13}C NMR ($CDCl_3$, δ in ppm): 217.3, 171.2, 168.2, 118.8, 63.4, 62.7, 50.3, 46.3, 37.1, 37.0, 36.8, 33.8, 31.9, 29.7, 29.6, 29.5, 29.4, 29.3, 29.0, 28.9, 27.6, 24.9, 22.7, 14.1.

FTIR: 2924.8, 2852.8, 2108.9, 1741.3, 1647.2, 1507.2, 1457.2, 1420.1, 1386.5, 1346.6, 1292.4, 1180.8, 1068.8, 384.8, 859.5, 804.1, 721.6.

ESI-MS [M+H$^+$] (in m/z): 623.0 (*Calculated* 623.2).

CDP-CC-N_3 was prepared similar to that of the CDP-SS-N_3 with 1,6-hexanediol as the starting material.

^{1}H NMR ($CDCl_3$, δ in ppm): 4.47 (t, 2H, COO*CH*$_2$CH$_2$), 4.37 (t, 2H, COO*CH*$_2$CH$_2$), 3.88 (s, 2H, C*H*$_2$N$_3$), 3.33 (t, 2H, C*H*$_2$S), 2.68-2.30 (m, 4H, C*H*$_2$C*H*$_2$), 1.89 (s, 3H, C(CN)C*H*$_3$), 1.80-1.55 (m, 4H), 1.50-1.22 (br, 22H), 0.89 (t, 3H, C*H*$_3$).

^{13}C NMR ($CDCl_3$, δ in ppm): 219.6, 171.5, 168.3, 119.0, 65.7, 64.9, 50.4, 46.4, 37.0, 33.9, 31.8, 29.8, 29.6, 29.5, 29.4, 29.3, 29.0, 28.5, 27.7,25.5, 25.4, 24.9, 22.7, 14.1.

FTIR: 2924.9, 2853.3, 2359.6, 2341.1, 2107.0, 1738.4, 1683.4, 1457.2, 1290.2, 1259.4, 1188.8, 1069.1, 857.9, 802.5, 721.1.

ESI-MS [M+H$^+$] (in m/z): 587.3 (*Calculated* 587.3).

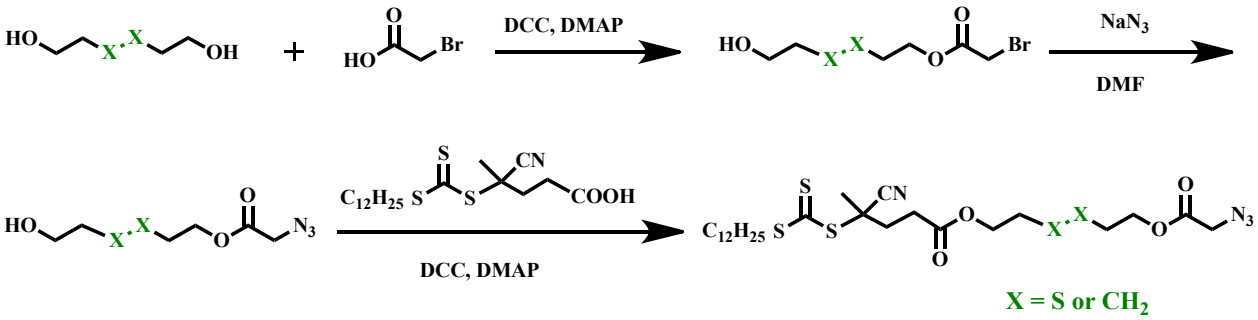

Scheme S1 Synthetic pathways for the azido-functionalized CDP-SS-N_3 and CDP-CC-N_3

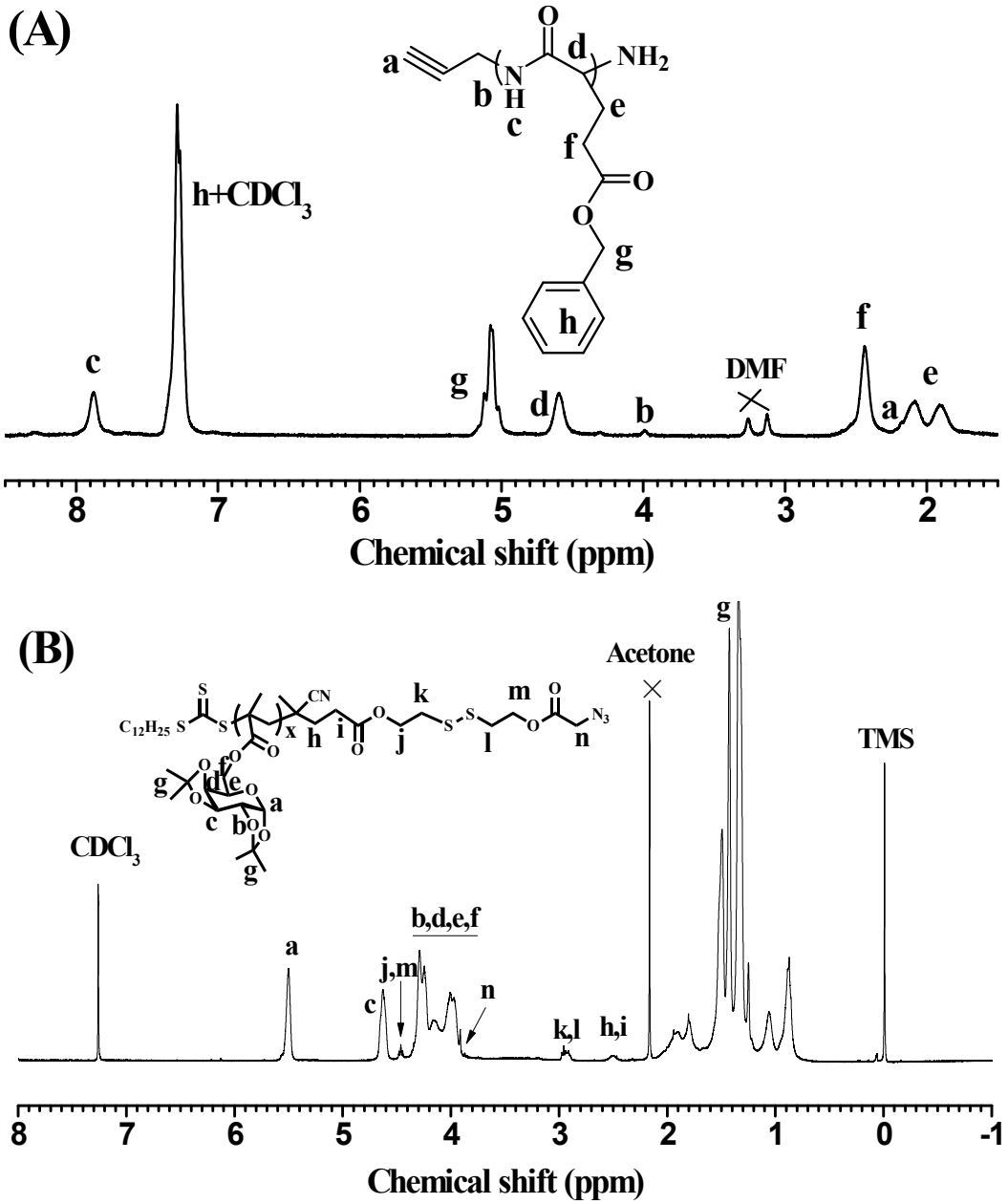

Fig. S1 ^{1}H NMR spectra of PBLG (A) in $CDCl_3$ with 15% TFA and PMAIpGP-*SS*-N_3 (B) homopolymer in $CDCl_3$.

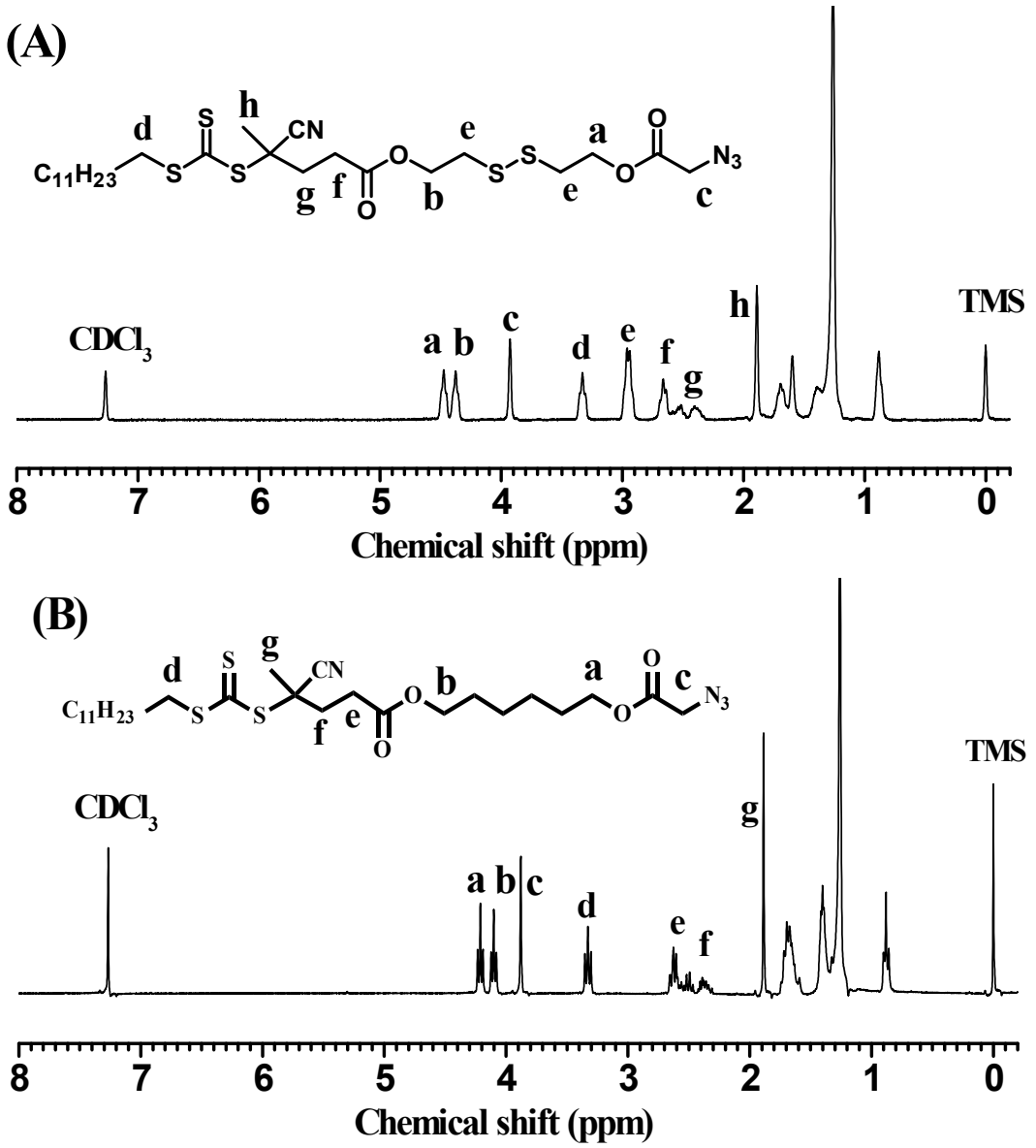

Fig. S2 ^{1}H NMR spectra of CDP-SS-N_3 (A) and CDP-CC-N_3 (B) in $CDCl_3$.

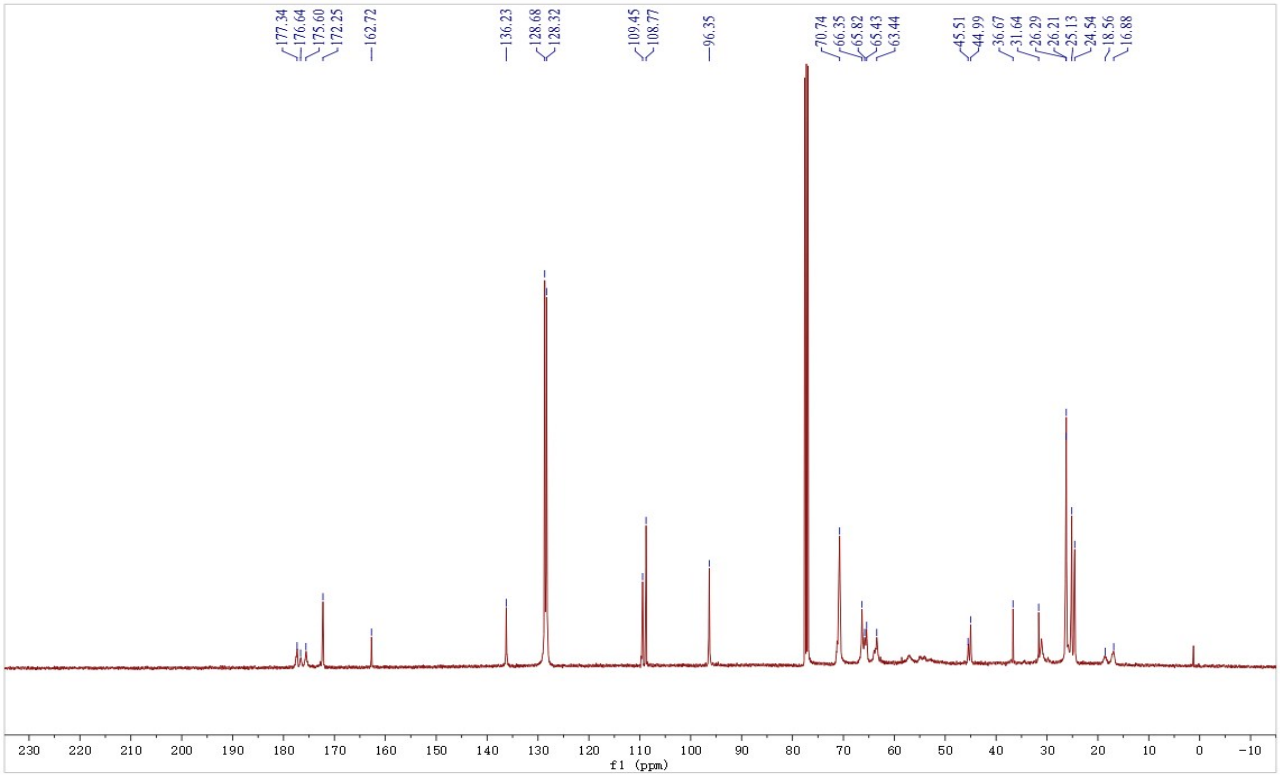

(A)

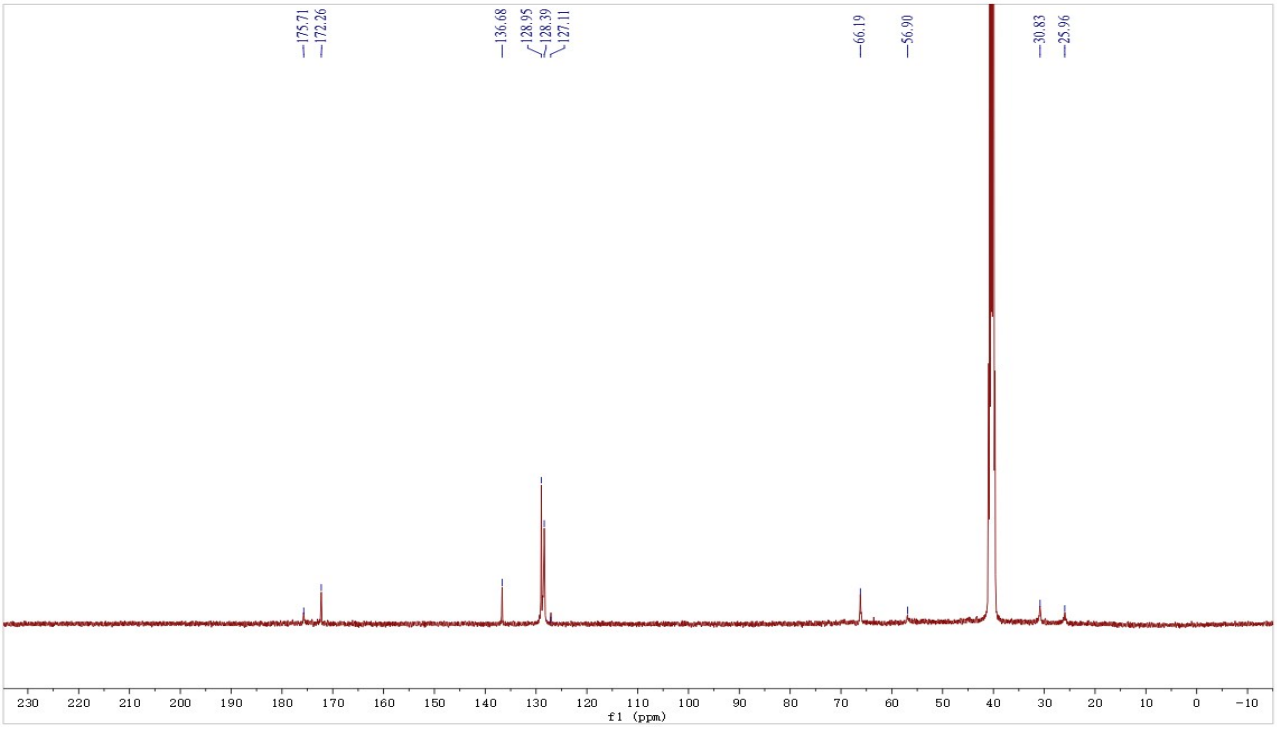

(B)

Fig. S3 ^{13}C NMR spectra of the synthesized PMAIpGP$_{27}$-*SS*-PBLG$_{40}$ in $CDCl_3$ (A) and its deprotected amphiphile PMAgala$_{27}$-*SS*-PBLG$_{40}$ in DMSO-d_6 (B)

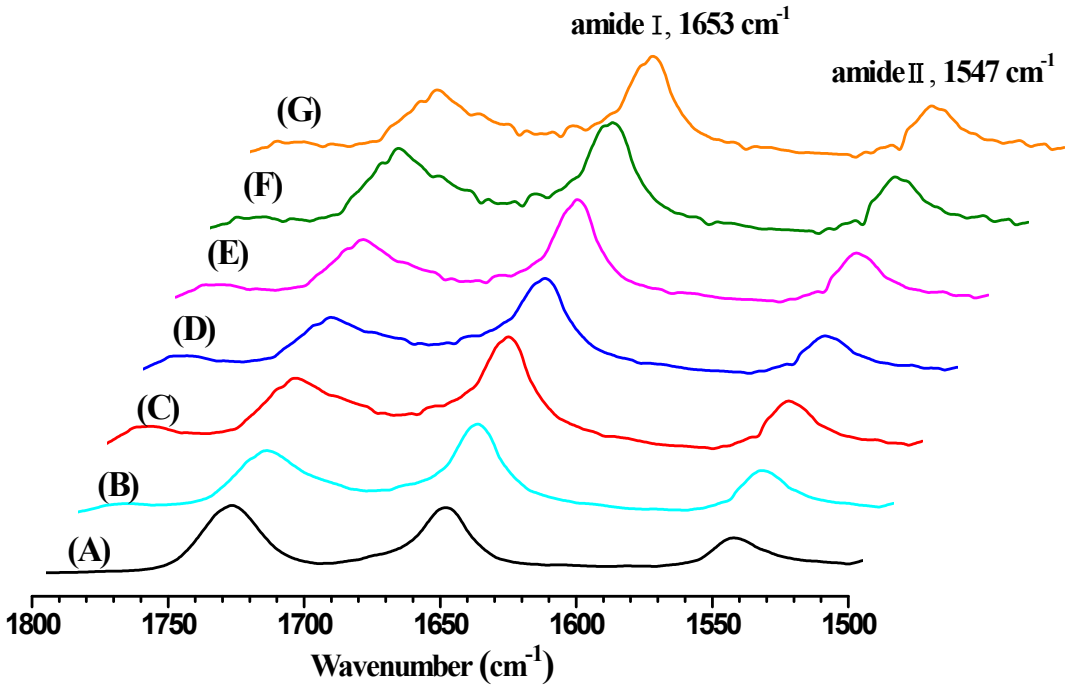

Fig. S4 Partial FTIR spectra for the synthesized PBLG homopolymer and diblock copolymers series. (A) $PBLG_{40}$, (B) $PMAIpGP_{27}$-*SS*-$PBLG_{40}$, (C) $PMAgala_{27}$-*SS*-$PBLG_{27}$, (D) $PMAgala_{27}$-*SS*-$PBLG_{30}$, (E) $PMAgala_{27}$-*SS*-$PBLG_{40}$, (F) $PMAgala_{27}$-*SS*-$PBLG_{50}$ and (G) $PMAgala_{27}$-*CC*-$PBLG_{30}$.

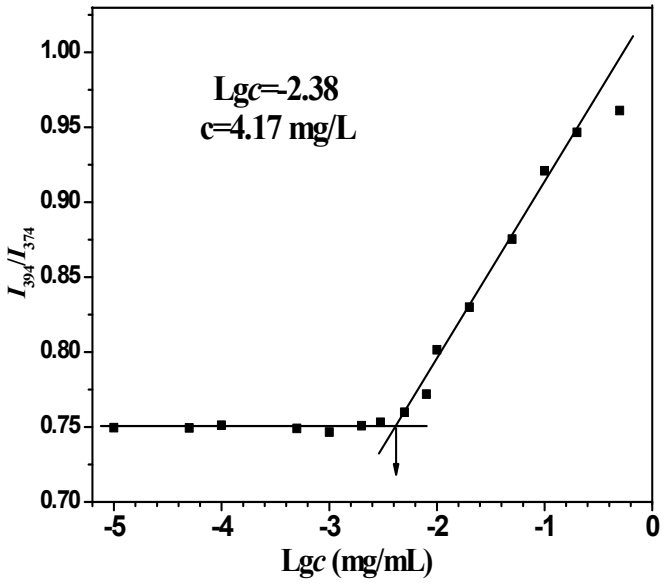

Fig. S5 Fluorescence intensity ratios (I_{394}/I_{374}) versus mass concentration for the PMAgala$_{27}$-*SS*-PBLG$_{30}$ in water.

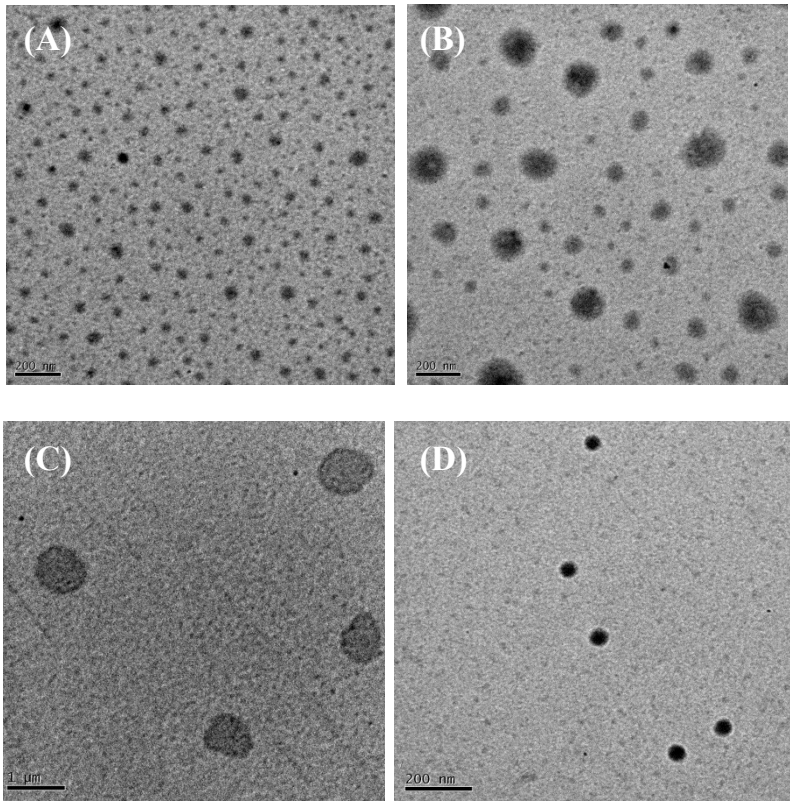

Fig. S6 TEM images for the self-assembled micelles prepared by PMAgala$_{27}$-*SS*-PBLG$_{27}$ (A), PMAgala$_{27}$-*SS*-PBLG$_{40}$ (B), PMAgala$_{27}$-*SS*-PBLG$_{50}$ (C) and PMAgala$_{27}$-*CC*-PBLG$_{30}$ (D).

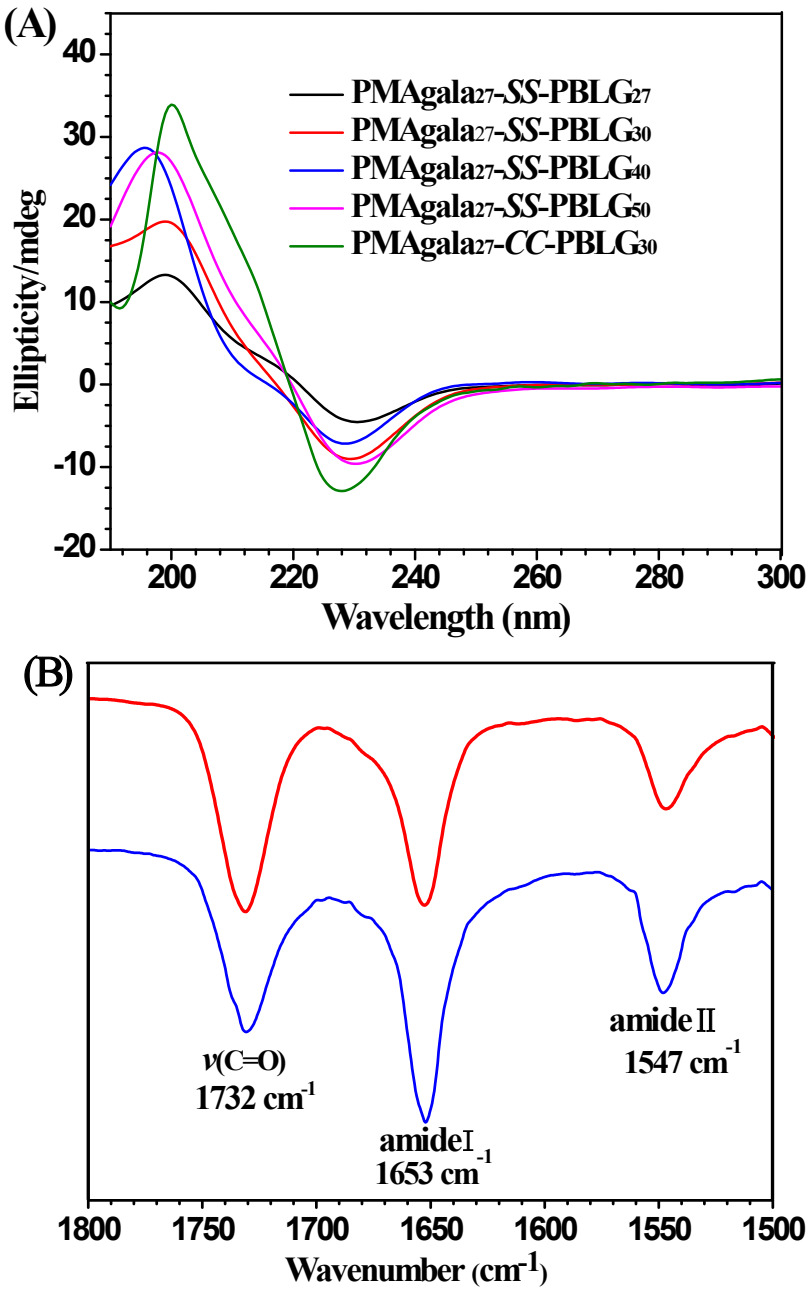

Fig. S7 CD spectra for the PMAgala-*b*-PBLG micelles in deionized water (A) and featured FTIR spectra (B) for the freeze-dried powders from the PMAgala$_{27}$-*SS*-PBLG$_{30}$ micelles solution (blue curve) and solids (red curve).

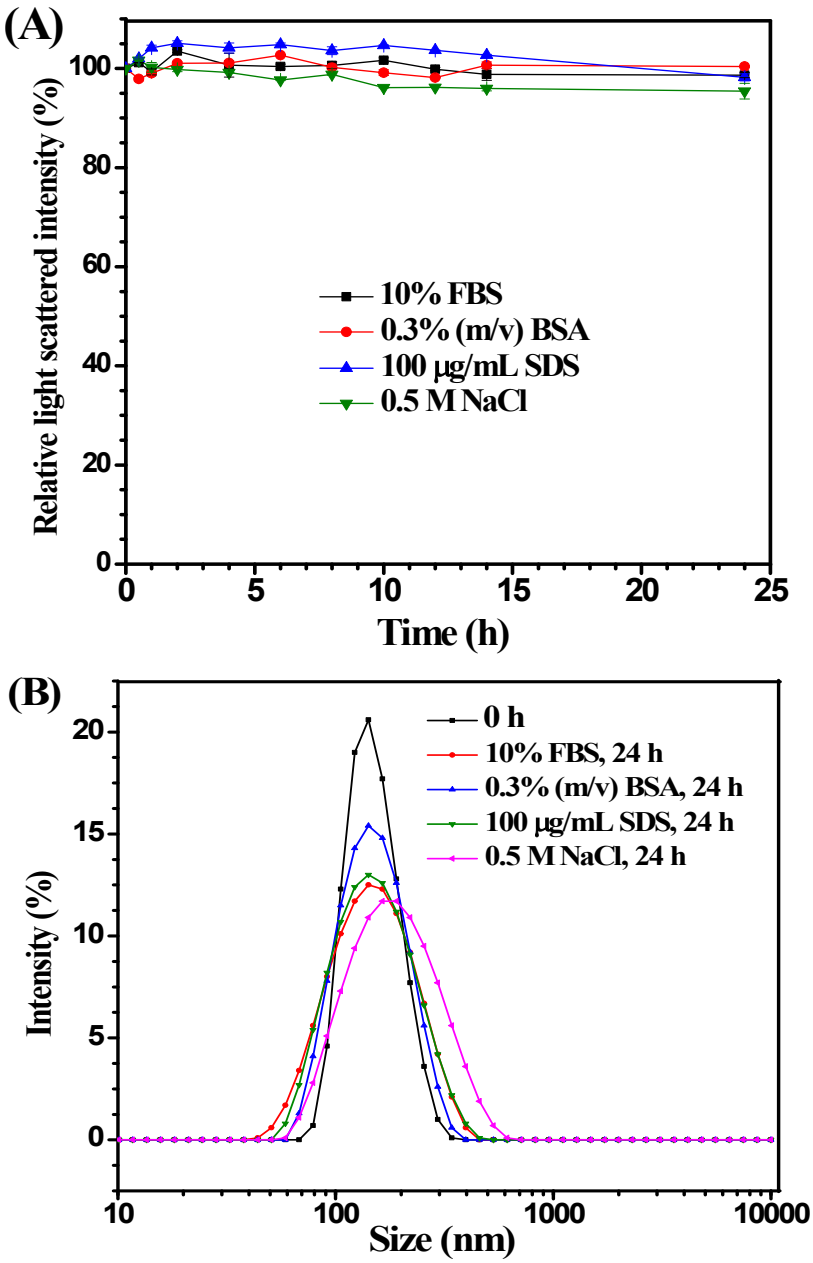

Fig. S8 Stability assay for the PMAgala$_{27}$-*SS*-PBLG$_{30}$ micelles by DLS in the presence of FBS, BSA, SDS or NaCl. (A) Time dependence of relative light scattered intensity. (B) Particle size change after 24 h incubation.

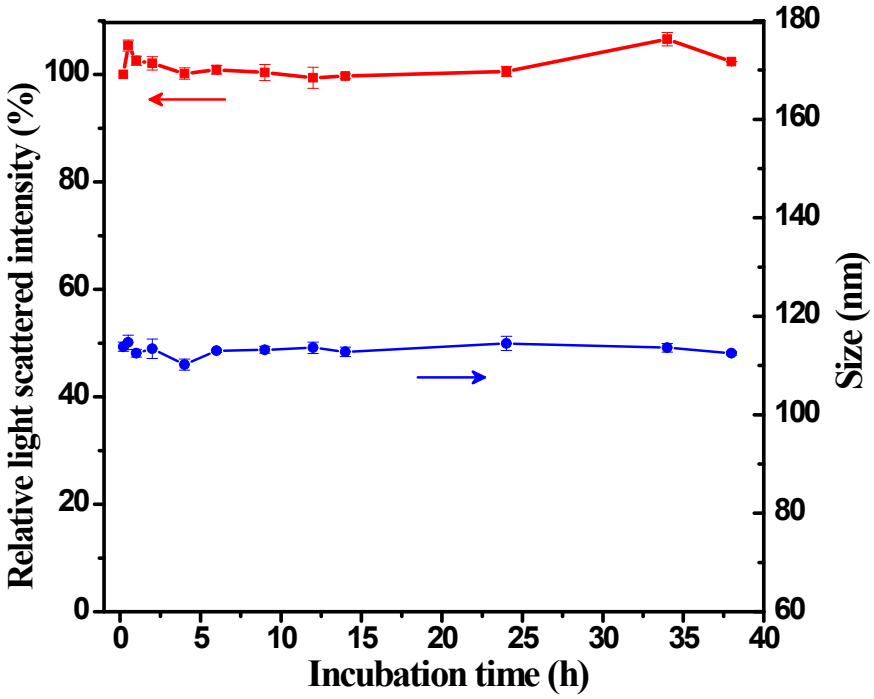

Fig. S9 Incubation time dependence of relative light scattered intensity and average particle size for the PMAgala$_{27}$-*CC*-PBLG$_{30}$ micelles in the presence of 10 mM GSH at 37℃.

Table S1 Characteristics of the DOX-loaded PMAgala-*b*-PBLG micelles

DOX–loaded Samples	Size (nm)	PDI	DOX Feed ratio (*wt* %)	DLC (%)	DLE (*wt* %)
PMAgala$_{27}$-*SS*-PBLG$_{30}$/DOX	153.7±1.37	0.174	10	92	9.27
PMAgala$_{27}$-*CC*-PBLG$_{30}$/DOX	168.0±2.36	0.159	10	94	9.46